

PACS numbers: 42.65.Ky; 42.70.Hj; 42.70.Qs
DOI: 10.1070/QE2005v035n01ABEH002836

Spatial and energy parameters of laser radiation and second harmonic upon self-frequency doubling

G.D. Laptev, A.A. Novikov, A.S. Chirkin

***Abstract*. The intracavity second-harmonic generation of laser radiation in an active nonlinear crystal is studied. The spatial distributions of the intensity and power of laser radiation and its second harmonic are calculated by the method of numerical simulations as functions of the parameters of the resonator, active nonlinear crystal, and pump. The analysis is performed for a periodically poled $Nd:Mg:LiNbO_3$ crystal taking diffraction into account.**

Keywords: *self-frequency doubling, active nonlinear crystals, periodically poled structure, diffraction, transverse mode structure*.

1. Introduction

Second harmonic generation (SHG) is the first nonlinear-optical process that was observed in laser beams [1, 2] and provided the basis for the development of a variety of directions in nonlinear optics. For example, the observation of excess fluctuations of the second harmonic at the initial stage of its generation stimulated the development of statistical phenomena in nonlinear optics [3 – 6]. Parametric amplification in optics was also first observed in the second-harmonic field [7, 8]. For the last forty years, the SHG process has been investigated in detail both theoretically and experimentally, and analysis of nonlinear-optical phenomena in monographs and textbooks begins conventionally from the description of this process.

The extension of applications of sources of coherent and non-classical light attracts interest both to new methods of optical frequency conversion and unconventional nonlinear-optical media. Among the latter, active nonlinear crystals (ANCs) have long attract attention [9, 10].

Interest in ANCs, in which rare-earth ions provide active (laser) properties, while a crystal matrix plays the role of a nonlinear medium, is related to the possibility of the development of compact solid-state laser systems, which generate radiation at the wavelengths that can be used in many applications such as optical communication, optical storage devices, medicine, etc. In ANCs, the so-called self-frequency conversion can occur, when lasing takes place simultaneously with nonlinear laser frequency conversion [10, 11]: self-frequency doubling [12 – 21], parametric self-frequency conversion [22, 23], and summation of the laser and pump frequencies [24 – 28].

We showed earlier [29] that the use of periodically poled active nonlinear crystals provides a further extension of the possibilities of ANCs to increase the number of nonlinear-optical processes involved. Periodically poled crystals (PPCs), which possess no active properties, have been already widely used in nonlinear optics and its applications [30 – 32], providing efficient quasi-phase-matched nonlinear-optical processes even when the usual phase-matching conditions for the interaction waves are not fulfilled.

To further improve self-frequency conversion laser systems and to increase the number of nonlinear-optical processes proceeding in ANCs, it is necessary to develop models that would adequately describe self-frequency conversion. At present, self-frequency conversion was investigated theoretically only in a few papers, and in most of them the plane wave approximation was used [33 – 35]. Only in papers [11, 36] the theory of self-frequency doubling was developed in the Gaussian beam approximation by neglecting the size of resonator mirrors. The approach developed below makes up for this gap.

The aim of this paper is to study the spatial structure of laser radiation and its second harmonic generated in a periodically poled ANC taking into account diffraction effects in a laser resonator. It is well known that the spatial structure of laser radiation (laser beams) can be adequately described only taking diffraction into account. Diffraction effects upon SHG should be taken into account if the so-called confocal parameter of the fundamental radiation is smaller than the length of a nonlinear crystal [9, 37]. In the case of intracavity SHG, when a nonlinear crystal is placed inside the laser cavity, the manifestations of diffraction in laser radiation and second-harmonic radiation can be considered separately. In this case, as a rule, a nonlinear crystal is oriented so that the confocal parameter is larger than the crystal length, which allows one to neglect diffraction over the crystal length. We study the case of crystal orientation when lasing and frequency doubling occur in the same crystal. The theory developed in the paper takes into account a number of factors determining the efficiency of the process under study. Apart from the

G.D. Laptev International Teaching and Research Laser Center, M.V. Lomonosov Moscow State University, Vorob'evy gory, 119992 Moscow, Russia; Tel.: (095) 939 22 28; Fax: (095) 939 31 13; e-mail: gdlaptev@hotbox.ru;
A.A. Novikov, A.S. Chirkin Department of Physics, M.V. Lomonosov Moscow State University, Vorob'evy gory, 119992 Moscow, Russia; e-mail: alexey_novikov@hotbox.ru, aschirkin@pisem.net

Received 20 July 2004; revision received 27 September 2004
Kvantovaya Elektronika **35** (1) 13 – 20 (2005)
Translated by M.N. Sapozhnikov

factors that are usually considered in theoretical papers, we took into account for the first time a finite size of resonator mirrors. The equations describing simultaneously lasing, nonlinear frequency conversion, and propagation of waves inside the resonator were solved by using computer simulations.

2. System of equations and the method of solution

Consider an ANC placed inside a resonator formed by two spherical mirrors. The crystal is pumped through one of the resonator mirrors (end pumping). The self-frequency doubling of laser radiation in this scheme is described by the system of equations

$$\pm\frac{\partial A_1^{\pm}}{\partial z}-\frac{\mathrm{i}}{2n_1k_1}\left(\frac{\partial^2 A_1^{\pm}}{\partial x^2}+\frac{\partial^2 A_1^{\pm}}{\partial y^2}\right)-\tan\rho_1\frac{\partial A_1^{\pm}}{\partial x}$$

$$=\frac{\eta A_1^{\pm}}{2(1+|A_1^{+}+A_1^{-}|^2)}-\frac{\alpha_1}{2}A_1^{\pm}+\mathrm{i}\varepsilon A_1^{\pm *}A_2^{\pm}\exp(\mp\mathrm{i}\Delta kz), \quad (1)$$

$$\pm\frac{\partial A_2^{\pm}}{\partial z}-\frac{\mathrm{i}}{2n_2k_2}\left(\frac{\partial^2 A_2^{\pm}}{\partial x^2}+\frac{\partial^2 A_2^{\pm}}{\partial y^2}\right)-\tan\rho_2\frac{\partial A_2^{\pm}}{\partial x}$$

$$=-\frac{\alpha_2}{2}A_2^{\pm}+\mathrm{i}\varepsilon(A_1^{\pm})^2\exp(\pm\mathrm{i}\Delta kz). \quad (2)$$

The system of equations (1), (2) is obtained by generalising equations for self-frequency doubling in the plane wave approximation [9] by adding the second derivatives of fields with respect to transverse coordinates describing diffraction effects and also taking into account the interference between counterpropagating waves in the resonator in the first term in the right-hand side of Eqn (1), which is responsible for amplification. Here, $A_{1,2}^{\pm}$ are the amplitudes of laser waves (subscript 1) and the second harmonic (subscript 2) propagating in the positive ('+') and negative ('−') directions of the z axis (all the amplitudes are normalised to $\sqrt{I_s}$, where I_s is the saturation intensity in the active medium); $\alpha_{1,2}$ is the coefficient of linear losses in the crystal (in intensity); $k_{1,2}$ is the wave number in vacuum; $\varepsilon=8\pi^2[2\pi I_s/(cn_1^2n_2)]^{1/2}d_{\mathrm{eff}}/\lambda$ is the coefficient of nonlinear coupling between the interacting waves; $n_{1,2}$ are the refractive indices of the crystal at the fundamental radiation frequency and second harmonic; c is the speed of light in vacuum; λ is the laser wavelength at the fundamental frequency; d_{eff} is the effective nonlinear coefficient; $\Delta k=2n_1k_1-n_2k_2$ is the phase mismatch between the interacting waves; $\rho_{1,2}$ is the angle between the wave and beam vectors; the parameter $\eta=\sigma_{\mathrm{las}}N(x,y,z)$ is the gain in the medium; σ_{las} is the cross section for the laser transition; $N(x,y,z)$ is the inversion population at the laser levels for a four-level system, whose dynamics is determined by the balance equation [38]

$$\frac{\mathrm{d}N}{\mathrm{d}t}=-N\left(\frac{1}{\tau_1}+\sigma_{\mathrm{p}}\frac{I_{\mathrm{p}}}{\hbar\omega_{\mathrm{p}}}+\sigma_{\mathrm{las}}\frac{I_{\mathrm{las}}}{\hbar\omega}\right)+\sigma_{\mathrm{p}}n\frac{I_{\mathrm{p}}}{\hbar\omega_{\mathrm{p}}}. \quad (3)$$

Here, σ_{p} is the pump absorption cross section; I_{p} and I_{las} are the pump and laser radiation intensities at frequencies ω_{p} and ω, respectively; n is the concentration of active ions; and τ_1 is the relaxation time of the upper level.

We are interested in a stationary case. Then, we obtain from (3), taking into account that $I_{\mathrm{las}}=I_s|A_1^{+}+A_1^{-}|^2$, $I_s=\hbar\omega/(\sigma_{\mathrm{las}}\tau_1)$, the inversion population

$$N(x,y,z)=$$

$$=\frac{\sigma_{\mathrm{p}}I_{\mathrm{p}}(x,y,z)n\tau_1}{1+\sigma_{\mathrm{p}}\tau_1I_{\mathrm{p}}(x,y,z)/(\hbar\omega_{\mathrm{p}})+|A_1^{+}(x,y,z)+A_1^{-}(x,y,z)|^2}. \quad (4)$$

The system of equations (1), (2) should be supplemented with boundary conditions at the resonator mirrors [39]:

$$A_{1,2}^{-}(x,y,L)=-[1-T_{1,2}(L)]^{1/2}A_{1,2}^{+}(x,y,L)$$

$$\times\exp\left(\mathrm{i}k_{1,2}\frac{x^2+y^2}{R_L}+\mathrm{i}2k_{1,2}L\right)Q_L(x,y), \quad (5)$$

$$A_{1,2}^{+}(x,y,0)=-[1-T_{1,2}(0)]^{1/2}A_{1,2}^{-}(x,y,0)$$

$$\times\exp\left(-\mathrm{i}k_{1,2}\frac{x^2+y^2}{R_0}\right)Q_0(x,y), \quad (6)$$

where $T_{1,2}(0)$ and $T_{1,2}(L)$ are the energy transmission coefficients of the left and right resonator mirrors for the laser wavelength (subscript 1) and second harmonic (subscript 2); L is the distance between the resonator mirrors; the exponential factors take into account a change in the phase of the waves after reflection from spherical mirrors; R_0 and R_L are the radii of curvature of the left and right mirrors, respectively; the functions $Q_0(x,y)$ and $Q_L(x,y)$ take into account a finite aperture of resonator mirrors. Below, we will consider circular mirrors, for which

$$Q_{0,L}(x,y)=\begin{cases}1 & \text{for} \quad x^2+y^2\leqslant a_{0,L}^2,\\ 0 & \text{for} \quad x^2+y^2>a_{0,L}^2,\end{cases}$$

where a_0 and a_L are the radii of the left and right resonator mirrors, respectively.

The system of equations (1)–(6) was transformed for the convenience of numerical calculations by making some assumptions. Thus, we assumed that the resonator mirrors and the distribution of the pump intensity have a cylindrical symmetry. In this case, the fields can be represented in the form of the $m_{1,2}$th angular harmonic $E_{1,2}^{\pm}(r,z)$

$$A_{1,2}^{\pm}(x,y,z)=E_{1,2}^{\pm}(r,z)\exp(\mathrm{i}m_{1,2}\varphi), \quad (7)$$

where φ is the polar angle.

We also assumed that the pump radiation has a Gaussian distribution

$$I_{\mathrm{p}}=I_{\mathrm{p}}(r,z)=\frac{P_{\mathrm{p}}}{\pi R^2(z)}\exp\left(-\frac{r^2}{R^2(z)}\right)\exp(-n\sigma_{\mathrm{p}}z), \quad (8)$$

where

$$R(z)=\left\{R_{\mathrm{p}}^2+\left[\frac{(z-z_{\mathrm{w}})c}{n_{\mathrm{p}}\omega_{\mathrm{p}}R_{\mathrm{p}}}\right]^2\right\}^{1/2} \quad (9)$$

is the radius of the Gaussian beam; P_{p} and R_{p} are the

power and radius of the pump beam at the ANC surface; z_w is the position of the beam waist in the crystal; n_p is the refractive index of the ANC at the pump wavelength; and the factor $\exp(-n\sigma_p z)$ takes into account absorption of the pump radiation in the active medium.

In experiments, as a rule, the ANC length is ~ 1 cm. At the same time, the confocal parameter for radiation inside the resonator is usually a few centimetres.

Therefore diffraction effects have no time to manifest themselves over the ANC length, and therefore we can calculate separately the propagation of radiation in the resonator (diffraction effect) and self-frequency conversion of this radiation.

During the propagation of radiation in the resonator formed by circular spherical mirrors, the fields at the resonator mirrors are related by the integral equations [40]

$$E_{1,2}^{+}(r_2, L) = \frac{\mathrm{i}^{m_{1,2}+1} k_{1,2}}{L_{1,2}} \int_0^{a_L} E_{1,2}^{+}(r_1, 0) J_{m_{1,2}}(k_{1,2} r_1 r_2 / L_{1,2})$$

$$\times \exp\left\{ -\frac{\mathrm{i}k_{1,2}}{2L_{1,2}} \left[\left(1 - \frac{L_{1,2}}{R_0}\right) r_1^2 + \left(1 - \frac{L_{1,2}}{R_L}\right) r_2^2 \right] \right\} r_1 \mathrm{d}r_1, \quad (10)$$

$$E_{1,2}^{-}(r_1, 0) = \frac{\mathrm{i}^{m_{1,2}+1} k_{1,2}}{L_{1,2}} \int_0^{a_0} E_{1,2}^{-}(r_2, L) J_{m_{1,2}}(k_{1,2} r_1 r_2 / L_{1,2})$$

$$\times \exp\left\{ -\frac{\mathrm{i}k_{1,2}}{2L_{1,2}} \left[\left(1 - \frac{L_{1,2}}{R_0}\right) r_1^2 + \left(1 - \frac{L_{1,2}}{R_L}\right) r_2^2 \right] \right\} r_2 \mathrm{d}r_2, \quad (11)$$

where $m_{1,2}$ is the order of the angular harmonic; $J_m(x)$ is the Bessel function of the mth order of the real argument; $L_{1,2} = L - L_0(n_{1,2} - 1)/n_{1,2}$; and L_0 is the ANC length. The curvature radii and transverse sizes of mirrors were taken into account in Eqns (10) and (11).

In numerical calculations of the resonator, we neglected a rapidly oscillating term in (4), which is related to the interference between counterpropagating waves in the resonator, i.e., we used the conventional approximation [39]

$$|A_1^{+} + A_1^{-}|^2 = |A_1^{+}|^2 + |A_1^{-}|^2 + 2\mathrm{Re}[A_1^{+} A_1^{-*} \exp(\mathrm{i}2k_1 z)]$$

$$\approx |A_1^{+}|^2 + |A_1^{-}|^2. \quad (12)$$

In addition, we assumed that $\rho_{1,2} = 0$, which is valid for extraordinary waves propagating along the optical axis or perpendicular to it. The latter often takes place in PPCs.

Finally, taking the above assumptions into account, we obtained from Eqns (1)–(6) the following equations describing self-frequency doubling of laser radiation in active nonlinear PPCs:

$$\pm \frac{\mathrm{d}E_1^{\pm}}{\mathrm{d}z} = \frac{\sigma_{las}\sigma_p I_p n \tau_1 E_1^{\pm}}{2(1 + \sigma_p \tau_1 I_p / \hbar\omega_p + |E_1^{+}|^2 + |E_1^{-}|^2)} - \frac{\alpha_1}{2} E_1^{\pm}$$

$$+ \mathrm{i}g(z)\varepsilon E_1^{\pm *} E_2^{\pm} \exp(\mp \mathrm{i}\Delta k z), \quad (13)$$

$$\pm \frac{\mathrm{d}E_2^{\pm}}{\mathrm{d}z} = -\frac{\alpha_2}{2} E_2^{\pm} + \mathrm{i}g(z)\varepsilon (E_1^{\pm})^2 \exp(\pm \mathrm{i}\Delta k z) \quad (14)$$

for $z_0 \leqslant z \leqslant z_0 + L_0$, where z_0 is the position of the left face of the crystal inside the resonator; $g(z)$ is the function describing a periodic variation in the sign of the nonlinear coupling coefficient in the PPC crystal. The system of equations (10), (11), (13), (14) with the boundary conditions

$$E_{1,2}^{-}(r, L) = [1 - T_{1,2}(L)]^{1/2} E_{1,2}^{+}(r, L), \quad (15)$$

$$E_{1,2}^{+}(r, 0) = [1 - T_{1,2}(0)]^{1/2} E_{1,2}^{-}(r, 0) \quad (16)$$

was used for numerical calculations of the transverse mode structure of laser radiation and second harmonic during self-frequency doubling. The functions $E_{1,2}^{\pm}(r, 0)$ and $E_{1,2}^{\pm}(r, L)$ are the solutions of this system of equations.

The scheme of the resonator used in the analysis is shown in Fig. 1. As in most experiments on self-frequency doubling, a crystal was placed near the left mirror of the resonator ($z_0 = 0$), which is plane ($R_0 = \infty$) and highly reflecting for the fundamental and second harmonic radiation [$T_{1,2}(0) = 0$]; the right mirror of the resonator is the output mirror. The mirrors are completely transparent for the pump radiation. The apertures of the plane mirror and ANC are assumed identical.

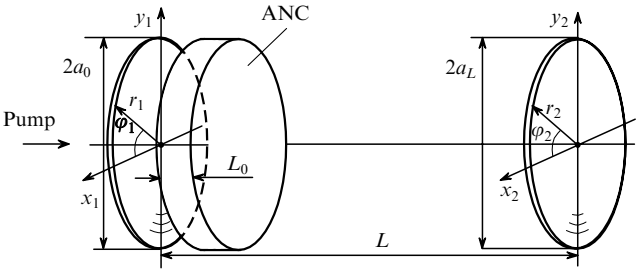

Figure 1. Scheme of a hemispherical resonator with an ANC for self-frequency doubling.

The system of equations (10), (11), (13)–(16) was solved numerically in the following way. First, arbitrary initial distributions of the laser field $E_1^{+}(r, 0)$ and the second-harmonic field $E_2^{+}(r, 0)$ at the left resonator mirror were specified. Then, the fields were numerically calculated from (13) and (14) after the propagation of radiation through the crystal from left to right by neglecting diffraction. The fulfilment of quasi-phase-matching conditions in the first order was assumed, which allowed us to replace the function $g(z)$ by its effective value $2/\pi$ (see, for example, [31]). Note that this replacement significantly reduces the computer calculation time when solving Eqns (13) and (14). Then, the fields behind the crystal were used for the numerical integration of Eqn (10) to find the fields $E_{1,2}^{+}(r, L)$ at the right resonator mirror. In this case, we took into account radiation losses due to the transmission of the right mirror [Eqn (15)]. The fields $E_{1,2}^{-}(r, 0)$ at the crystal surface were calculated by the numerical integration of Eqn (11). Then, the fields propagated through the crystal from right to left were calculated numerically from Eqns (13) and (14). As a result, taking relation (16) into account, we found again the spatial distribution of the fields at the left resonator mirror, and the above sequence of operations was repeated. The numerical calculation ended when the spatial distribution of the fields after the next round trip in the resonator became

identical with a high specified accuracy to the field distribution after the previous round trip [41]. Not also that the spatial distributions of the fields obtained by solving numerically the system of equations (10), (11), (13)–(16) remained the same after the variation of the initial distribution of the fields. The spatial distributions of the laser and second-harmonic fields found in this way correspond to the stationary regime of self-frequency doubling.

3. Results and discussion

We present in this section the results of numerical solution of the system of equations (10), (11), (13)–(16) for self-frequency doubling in an active nonlinear $Nd:Mg:LiNbO_3$ PPC. We reported the experimental study of self-frequency doubling in this crystal in [42]. The periodically poled structure of the $Nd:Mg:LiNbO_3$ crystal allows us to perform the ee–e type quasi-phase-matched nonlinear-optic interaction, which permits the use of the maximum nonlinear coefficient d_{33}. The results of calculations of the spatial intensity and power distributions are presented in Figs 2–9, the intensities being normalised to their maxima.

We used in calculations the values of parameters that were close to the experimental values: the length of the active nonlinear PPC was 0.5 cm, the pump wavelength $\lambda_p = 810$ nm, the pump absorption cross section $\sigma_p = 5.4 \times 10^{-20}$ cm^2, the pump power $P_p = 1$ W, the pump beam radius in the crystal $R_p = 50$ μm [we assumed that the confocal parameter of the pump beam, which is approximately 1.6 cm for the above values of parameters, is greater than the crystal length, i.e., $z_w = 0$ in (9)], the laser wavelength was 1084 nm, the laser transition cross section $\sigma_{las} = 18 \times 10^{-20}$ cm^2, the relaxation time of the inversed population $\tau_1 = 10^{-4}$ s, the concentration of active ions $n = 5 \times 10^{19}$ cm^{-3}, the effective nonlinear coefficient $d_{eff} = 2d_{33}/\pi = 22$ pm V^{-1}, the refractive indices $n_1 = 2.15$ and $n_2 = 2.22$ at the wavelengths 1084 and 542 nm, respectively, linear loss coefficients $\alpha_1 = 0.1$ cm^{-1} and $\alpha_2 = 0.3$ cm^{-1}, and the resonator length $L = 20$ cm. One of the resonator mirrors was plane ($R_0 = \infty$), while the radius of curvature of another mirror was $R_L = 20$ cm, i.e., the resonator was hemispherical, the diameters of the resonator mirrors were 1 cm, the mirrors had the 100 % reflectivity at a wavelength of 1084 nm, the plane mirror also had the 100 % reflectivity at the second-harmonic wavelength, while the output mirror was completely transparent for the second-harmonic radiation. The calculations were performed for the fundamental transverse mode ($m_{1,2} = 0$). The accuracy of calculation of the spatial distribution of the fields was $\delta = 10^{-8}$. The values of other parameters are indicated in figure captions. Note that in Figs 2–6, 8, 9, the laser output power is indicated at the fundamental frequency in the resonator with highly reflecting mirrors at this frequency.

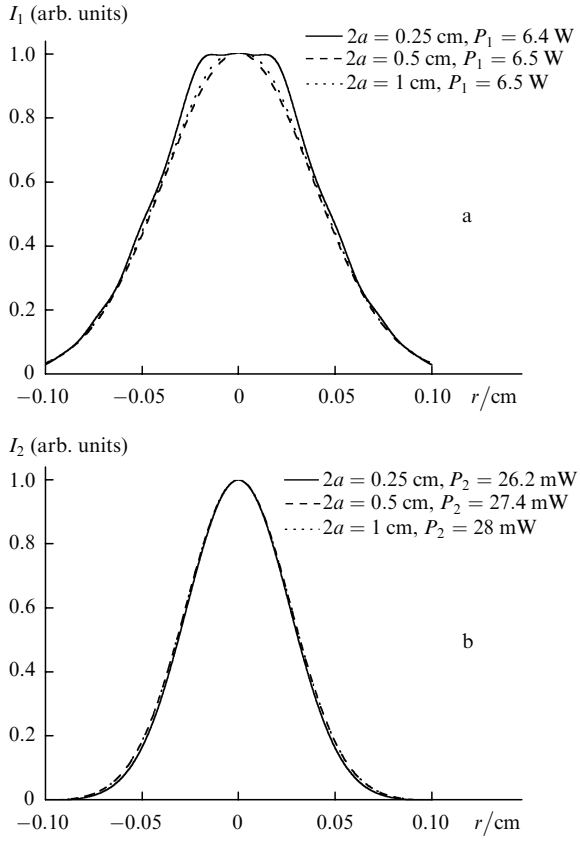

Figure 2. Normalised spatial distributions of the laser radiation intensity I_1 (a) at the output mirror and the second-harmonic intensity I_2 (b) at the resonator output for different diameters of resonator mirrors $2a_0 = 2a_L = 2a$ and powers of laser radiation P_1 and second harmonic P_2. The resonator length is $L = 20$ cm, the radius of curvature of the output mirror is $R_L = 20$ cm, the pump power is $P_p = 1$ W, the pump-beam radius is $R_p = 50$ μm, and the ANC length is $L_0 = 0.5$ cm.

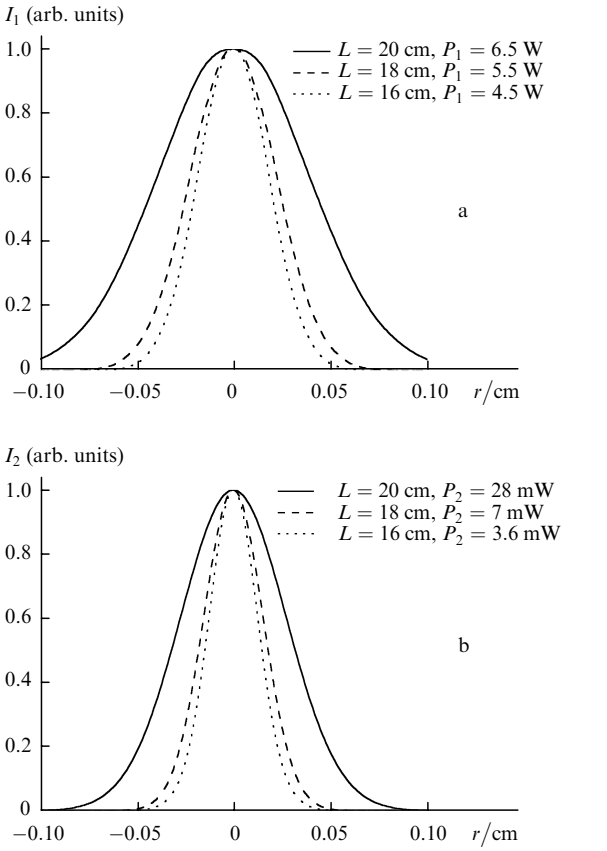

Figure 3. Same as in Fig. 2 for different lengths L of the resonator and different powers of laser radiation P_1 (a) and second harmonic P_2 (b); $2a = 1$ cm, $R_L = 20$ cm, $P_p = 1$ W, $R_p = 50$ μm, $L_0 = 0.5$ cm.

The results presented in Figs 2–6 depend on the action of three processes: diffraction, lasing, and nonlinear frequency conversion. As expected, the transverse size of the second-harmonic beam is always smaller than that of the fundamental beam.

One can see from Fig. 2 that the greater the diameter of the resonator mirrors, the less the effect of diffraction from the mirror edges on the transverse intensity distribution of laser radiation, whereas the intensity distribution of the second-harmonic radiation almost does not change. In our opinion, this is explained by the fact that the second-harmonic beam is narrower than the fundamental beam, so that the spatial distribution of the second-harmonic intensity is less sensitive to diffraction at the resonator mirror edges. According to Fig. 3, as the distance between the resonator mirrors is decreased, i.e., when the resonator is detuned from a hemispherical resonator, the transverse sizes of the laser and second-harmonic beams decrease somewhat, whereas their powers decrease substantially. This is explained by a decrease in the role of diffraction and of contribution from the active medium. This means that, when the separation between the resonator mirrors is constant, an increase in the radius of curvature of the output mirror should result in a similar effect.

It follows from Fig. 4 that when the resonator strongly differs from a hemispherical resonator, the spatial structure of laser radiation becomes rather complex, while the output power considerably decreases.

Figure 5 shows the dependence of the spatial structure of the fundamental and second-harmonic radiation at the fixed pump power on the pump-beam radius varied from 10 to 100 μm. When the pump-beam radius is small (10 μm), the observed spatial structure of fundamental radiation is determined by the fact that the transverse size of the gain region of the crystal is smaller that that of a mode of the empty resonator, i.e., the pump is used inefficiently. As the pump-beam radius is increased up to 50 μm, the output power increases, while the spatial intensity distribution becomes smoother, i.e., the pump radiation is used more efficiently. As R_p is further increased, the spatial intensity distribution does not change, while the output power decreases, which shows that the pump radiation again is used inefficiently. Therefore, there exists the optimal pump-beam radius at which the radiation power at the fundamental frequency is maximal. Figure 5 shows that this radius also provides the maximum second-harmonic power. Our calculations also showed that a change in the pump power does not change the spatial structure of the fundamental and second-harmonic radiation fields.

Our analyses shows that in the region of values of parameters considered in the paper the situation always takes place when a variation of some of the parameters causes a strong change in the spatial structure of laser radiation field, whereas the spatial structure of the second-harmonic field changes only weakly (Figs 2 and 5). Note that the spatial distributions of the laser radiation and second-harmonic fields have a nearly Gaussian profile in a broad range of values of parameters. At the same time, there exist the values of parameters at which the spatial distribution of the second-harmonic intensity strongly differs from a Gaussian due to a combined action of the saturation

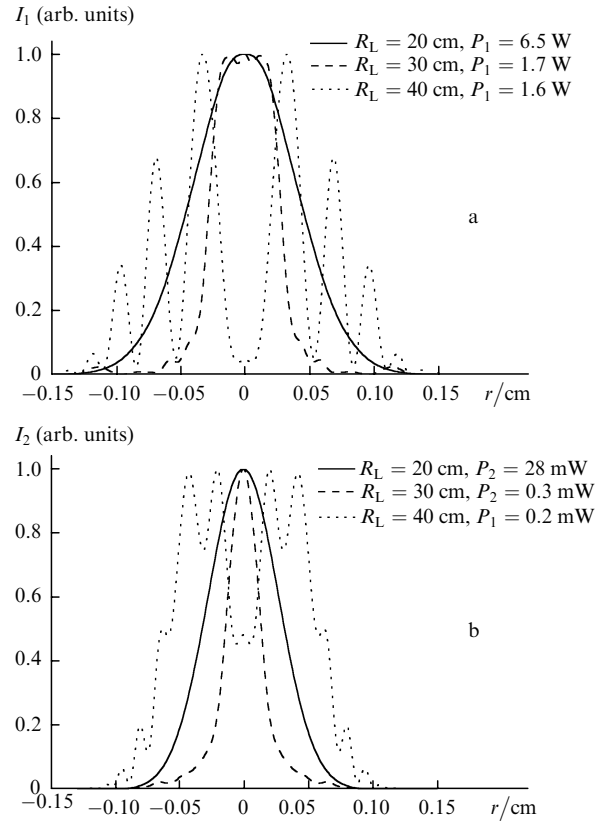

Figure 4. Same as in Fig. 2 for different radii of curvature of the output mirror and different powers of laser radiation P_1 (a) and second harmonic P_2 (b); $2a = 1$ cm, $L = 20$ cm, $P_p = 1$ W, $R_p = 50$ μm, $L_0 = 0.5$ cm.

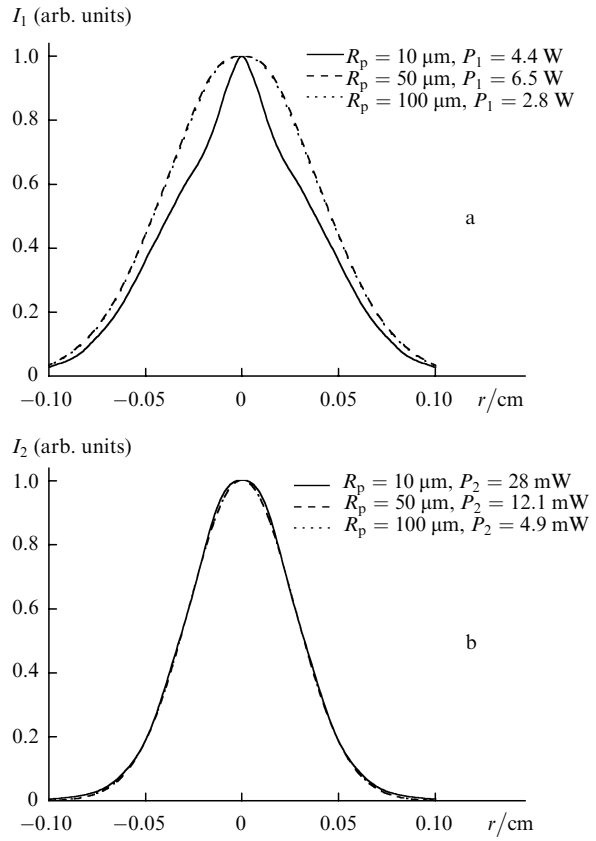

Figure 5. Same as in Fig. 2 for different radii R_p of the pump beam and different powers of laser radiation P_1 (a) and second harmonic P_2 (b); $2a = 1$ cm, $L = 20$ cm, $R_L = 20$ cm, $P_p = 1$ W, $L_0 = 0.5$ cm.

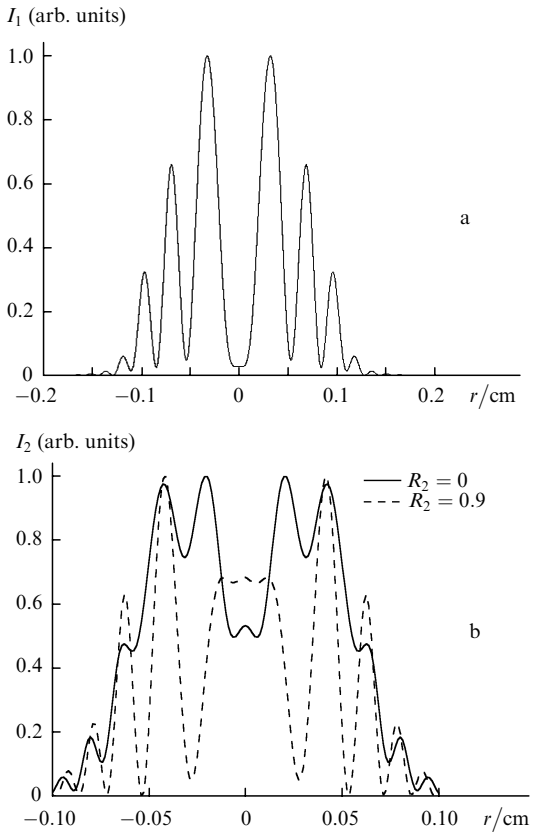

Figure 6. Same as in Fig. 2 for reflectivity R_2 of the output mirror for the second harmonic equal to 0 and 0.9; $2a = 0.5$ cm, $L = 20$ cm, $R_L = 40$ cm, $P_p = 1$ W, $R_p = 50$ μm.

of the active medium, nonlinear interaction of the waves, and diffraction (Figs 4 and 6).

We also compared the spatial intensity distributions of fundamental radiation in the case of self-frequency doubling and in the absence of SHG. Our calculations showed that the spatial distributions of fundamental radiation in these two cases slightly differ from each other, only the output powers being different. In other words, even a great energy transfer to the second harmonic does not affect substantially the spatial distribution of the fundamental radiation intensity. At the same time, the spatial distribution of the second-harmonic intensity depends not only on the intensity distribution of fundamental radiation but on the other parameters of the problem as well. For example, Fig. 6 demonstrates two spatial distributions of the second-harmonic intensity calculated for different reflectivities of the resonator mirrors at the second-harmonic wavelength, which are substantially different, whereas the spatial distributions of the fundamental radiation intensity are virtually the same.

Figures 7–9 present some power characteristics studied in the paper. One can see from Fig. 7 that there exists the optimal reflectivity of the output mirror of the resonator at which the output power of the second harmonic is maximal. Similar results for crystals of lengths 0.1 and 0.5 cm were obtained in the case of plane waves [35]. At the same time, the dependence obtained for a crystal of length 0.9 cm differs from these dependences in the case of plane waves. One can also see that to increase the second-harmonic power in the case of ANCs of a smaller length, it is

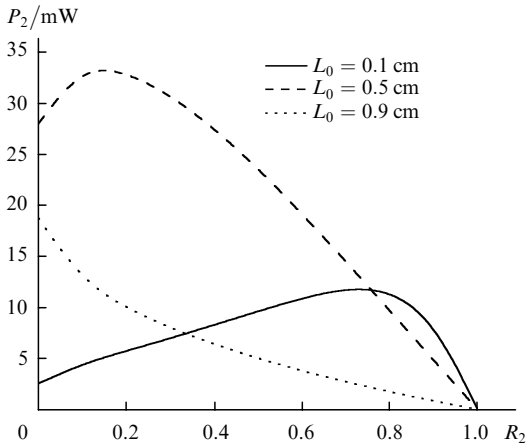

Figure 7. Dependences of the second-harmonic power P_2 at the resonator output on the reflectivity R_2 of the output mirror for the second harmonic for different lengths of the ANC; $2a = 1$ cm, $L = 20$ cm, $R_L = 20$ cm, $P_p = 1$ W, $R_p = 50$ μm.

expedient to use a higher-Q (for the second-harmonic radiation) resonator.

Figure 8 shows the dependences of the power of laser radiation and its second-harmonic at the resonator output on the pump power for crystals of different lengths. The threshold pump power for the parameters of the crystal and resonator considered in the paper was 0.2–0.4 W. One can see that the dependence of the laser radiation power on the

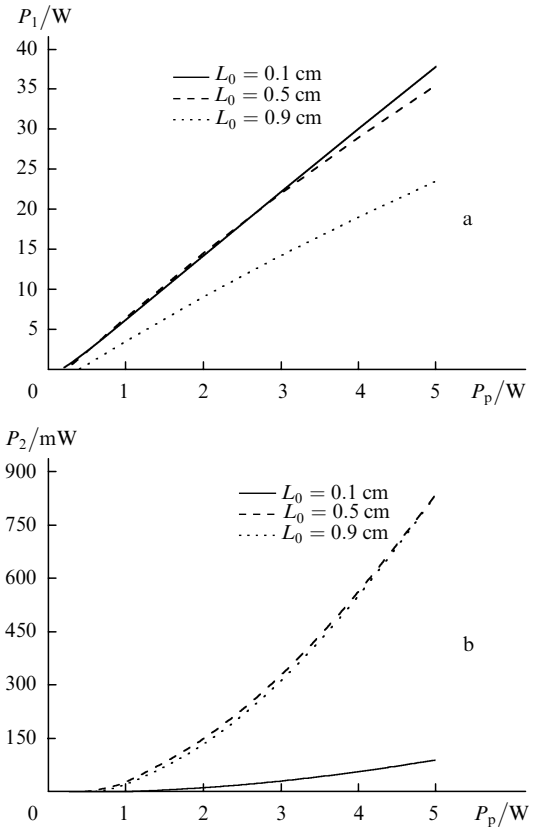

Figure 8. Dependences of the laser radiation power P_1 inside the resonator (a) and the output second-harmonic power P_2 (b) on the pump power P_p for different ANC lengths; $2a = 1$ cm, $L = 20$ cm, $R_L = 20$ cm, $R_p = 50$ μm.

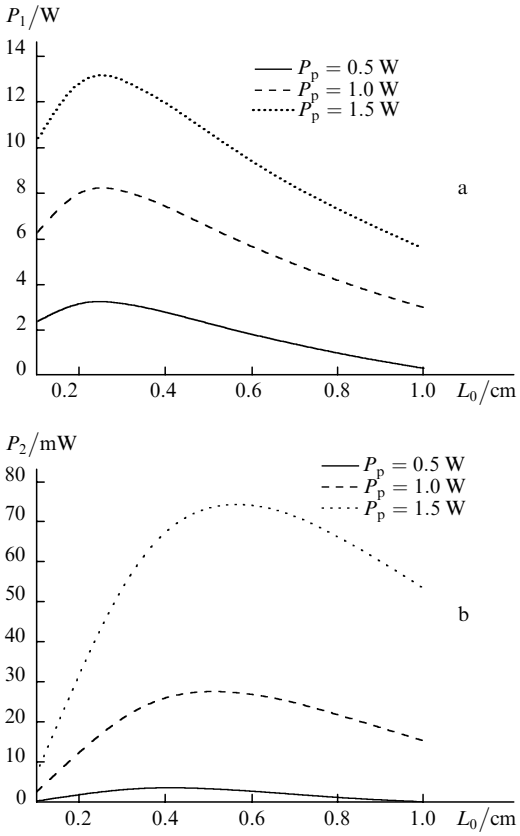

Figure 9. Dependences of the laser radiation power P_1 inside the resonator (a) and the output second-harmonic power P_2 (b) on the ANC length L_0 for different pump powers P_p; $2a = 1$ cm, $L = 20$ cm, $R_L = 20$ cm, $R_p = 50$ μm.

pump power at low pump powers is linear, while the second-harmonic power increases quadratically, which is confirmed by experiments on self-frequency doubling [12–21]. However, it follows from Fig. 8 that at sufficiently high pump powers the first dependence deviates from linear and the second one from quadratic. This is explained by the fact that at high pump powers, a great amount of energy transfers from the laser wave to the second-harmonic wave due to nonlinear conversion, i.e., the reverse effect of the second-harmonic wave on the fundamental wave takes place.

Figure 9 illustrates the dependences of the laser radiation power and its second harmonic on the ANC length for different pump powers. One can see that there exists the optimal crystal length for each pump power at which the second-harmonic power at the resonator output is maximal, the optimal radiation power depending on the pump power. The position of the optimum is obviously determined by the competition between processes of pump absorption, gain, losses, and nonlinear interaction in the crystal.

4. Conclusions

We have studied self-frequency doubling of laser radiation in an active nonlinear Nd : Mg : $LiNbO_3$ PPC taking into account many specific features of the realisation of this process, including a finite size and the radius of curvature of the resonator mirrors. We have analysed the influence of the parameters of the crystal, pump, and resonator on the formation of the transverse spatial structure of the field in the resonator. It has been found that second harmonic generation, affecting the fundamental radiation power, only weakly affects the spatial distribution of its intensity. It is shown that second harmonic can be efficiently generated by selecting parameters appropriately.

Acknowledgements. The authors thank S.G. Grechin, V.P. Kandidov, and T.Yu. Cherezova for useful discussions. This work was partially supported by the INTAS (Grant No. 01-2097).

References

1. Franken P.A., Hill A.E., Peters C.W., Weinreich G. *Phys. Rev. Lett.*, **7**, 118 (1961).
2. Akhmanov S.A., Kovrigin A.I., Khokhlov R.V., Chunaev O.N. *Zh. Eksp. Teor. Fiz.*, **45**, 1336 (1963).
3. Ducuing J., Bloembergen N. *Phys. Rev. A*, **133**, 1493 (1964).
4. Akhmanov S.A., Chirkin A.S. *Vestn. Mosk. Univ., Ser. Fiz. Astron.*, **5**, 79 (1965).
5. Akhmanov S.A., Kovrigin A.I., Chirkin A.S., Chunaev O.N. *Zh. Eksp. Teor. Fiz.*, **49**, 829 (1966).
6. Akhmanov S.A., Chirkin A.S. *Statisticheskie yavleniya v nelineinoi optike* (Statistical Phenomena in Nonlinear Optics) (Moscow: Izd. Moscow State University, 1971).
7. Giordmaire J.A., Miller R.C. *Phys. Rev. Lett.*, **14**, 973 (1965).
8. Akhmanov S.A., Kovrigin A.I., Fadeev V.V., Khokhlov R.V. *Pis'ma Zh. Eksp. Teor. Fiz.*, **2**, 300 (1965); Akhmanov S.A., Chunaev O.N., Fadeev V.V., Khokhlov R.V., Klyshko D.N., Kovrigin A.I., Piskarskas A.S. *Proc. Symp. Mod. Optics* (New York, NY, Brooklyn, 1967) p. 343.
9. Dmitriev V.G., Tarasov L.V. *Prikladnaya nelineinaya optika* (Applied Nonlinear Optics) (Moscow: Radio i Svyaz', 1982).
10. Laptev G.D., Novikov A.A., Chirkin A.S. *J. Russian Laser Research*, **23**, 183 (2002).
11. Brenier A. *J. Luminesc.*, **91**, 121 (2000).
12. Bartschke J., Boller K.-J., Wallenstein R., Klimov I.V., Tsvetkov V.B., Shcherbakov I.A. *J. Opt. Soc. Am. B*, **14**, 3452 (1997).
13. Jaque D., Capmany J., Carsia Sole J., Luo Z.D., Jiang A.D. *J. Opt. Soc. Am. B*, **15**, 1656 (1998).
14. Shengzi Z., Xingyu Z., Qingpu W., Songtao W., Lianke S., Shaojun Z., Guangtao Y., Zhenya Z. *Opt. Laser Technol.*, **30**, 239 (1998).
15. Dekker P., Huo Y., Dawes J.M., Piper J.A., Wang P., Lu B.S. *Opt. Commun.*, **151**, 406 (1998).
16. Zhang H.J., Meng X.L., Zhu L., Wang C.Q., Cheng R.P., Yu W.T., Zhang S.J., Sun L.K., Chow Y.T., Zhang W.L., Wang H., Wong K.S. *Opt. Commun.*, **160**, 273 (1999).
17. Chai B.H.T., Richardson M., Shah L., Eichenholz J., Peale R., Hammons D., Ye Q., Chin A. *Opt. Commun.*, **164**, 33 (1999).
18. Wang C.Q., Chow Y.T., Gambling W.A., Zhang S.J., Cheng Z.X., Shao Z.S., Chen H.C. *Opt. Commun.*, **174**, 471 (2000).
19. Maunier C., Doulan J.L., Aka G., Landais J., Antic-Fidancev E., Moncorge R., Vivien D. *Opt. Commun.*, **184**, 209 (2000).
20. Dekker P., Dawes J.M., Piper J.A., Liu Y., Wang J. *Opt. Commun.*, **195**, 431 (2001).
21. Burns P.A., Dawes J.M., Dekker P., Piper J.A., Li J., Wang J. *Opt. Commun.*, **207**, 315 (2002).
22. Barraco L., Grisard A., Lallier E., Bourdon P., Pocholle J.-P. *Opt. Lett.*, **27**, 1540 (2002).
23. Capmany J., Callejo D., Bermudez V., Dieguez E., Artigas D., Torner L. *Appl. Phys. Lett.*, **79**, 293 (2001).
24. Jaque D., Capmany J., Garsia Sole J. *Appl. Phys. Lett.*, **73**, 3659 (1998).
25. Jaque D., Garcia Sole J., Boulon G., Brenier A. *Opt. Mater.*, **13**, 311 (1999).
26. Jaque D. *Journal of Alloys and Compounds*, **323–324**, 204 (2001).
27. Mougel F., Kahn-Harari A., Vivien D., Aka G. *Opt. Mater.*, **13**, 293 (1999).

28. Kravtsov N.V., Laptev G.D., Naumova I.I., Novikov A.A., Firsov V.V., Chirkin A.S. *Kvantovya Elektron.*, **32**, 923 (2002) [*Quantum Electron.*, **32**, 923 (2002)].
29. Laptev G.D., Novikov A.A., Chirkin A.S. *Pis'ma Zh. Eksp. Teor. Fiz.*, **78**, 45 (2003).
30. Fejer M.M., Magel G.A., Jundt D.H., Byer R.L. *IEEE J. Quantum Electron.*, **28**, 2631 (1992).
31. Chirkin A.S., Volkov V.V., Laptev G.D., Morozov E.Yu. *Kvantovaya Elektron.*, **30**, 847 (2000) [*Quantum Electron.*, **30**, 847 (2000)].
32. Byer R.L. *J. Nonlinear Optical Physics & Materials*, **6**, 549 (1997).
33. Dmitriev V.G., Zenkin V.A., Kornienko N.E., Ryzhkov A.I., Strizhevskii V.L. *Kvantovaya Elektron.*, **5**, 2416 (1978) [*Sov. J. Quantum Electron.*, **8**, 1356 (1978)].
34. Karpenko S.G., Strizhevskii V.L. *Kvantovaya Elektron.*, **6**, 437 (1979) [*Sov. J. Quantum Electron.*, **9**, 265 (1979)].
35. Laptev G.D., Novikov A.A. *Kvantovaya Elektron.*, **31**, 981 (2001) [*Quantum Electron.*, **31**, 981 (2001)].
36. Brenier A. *Opt. Commun.*, **141**, 221 (1997).
37. Akhmanov S.A., Kovrigin A.I., Sukhorukov A.P., in *Quantum Electronics. A treatise* (New York: Acad. Press, 1975) Vol. 1, p. 475.
38. Svelto O. *Principles of Lasers* (New York: Plenum Press, 1982; Moscow: Mir, 1984).
39. Elkin N.N., Napartovich A.P. *Prikladnaya optika lazerov* (Applied Optics of Lasers) (Moscow: TsNII Atominform, 1989).
40. Li T. *Bell System Technical J.*, **44**, 917 (1965).
41. Bykov V.P., Silichev O.O. *Lazernye rezonatory* (Laser Resonators) (Moscow: Fizmatlit, 2003).
42. Laptev G.D., Novikov A.A., Chirkin A.S., Firsov V.V., Kravtsov N.V. *Proc. SPIE Int. Soc. Opt. Eng.*, **4268**, 26 (2001).